UDC 681.7:535.5
DOI: 10.20535/2077-7264.2(76).2022.265683

© O. H. Ushenko, Doctor of physics and mathematics of science, Professor, O. V. Dubolazov, Doctor of physics and mathematics of science, Associate professor, M. P. Horskyi, PhD in physics and mathematics science, Associate professor, I. V. Soltys, PhD in physics and mathematics science, Associate professor, Chernivtsi National University, Chernivtsi, Ukraine

3D COMPUTER ALGORITHMS FOR DIGITAL RECONSTRUCTION OF THE POLYCRYSTALLINE STRUCTURE OF POLYGRAPHIC POLYMERS

Proposed and substantiated a method for 3D Mueller-matrix reproduction of the distributions of parameters of linear and circular birefringence and dichroism of partially depolarizing polymer films in publishing and printing business.

Keywords: 3D reconstruction; polymer film; Mueller matrix; depolarization.

Introduction

At present, methods and means of Mueller-matrix polarimetric (MMP) diagnostics of the structure of polymer films are being actively developed in optics. It includes a number of original directions: the study of scattering matrices [1–5] and Mueller-matrix polarimetry [6–10]. The further development and generalization of the methods of MMP 3D polycrystalline structure of films with different multiplicity of light scattering, or different depolarizing ability is urgent.

Our work is aimed at developing a Mueller-matrix mapping method for reconstructing the distributions of the optical anisotropy parameters of partially depolarizing films of various polymers.

Methods

It is based on the use of a reference wave of laser radiation, which in the scheme of an optical interferometer is superimposed on a polarization-inhomogeneous image of a polymer film. The resulting interference pattern is recorded using a digital camera. Using diffraction integrals, the digital holographic reproduction of the distributions of the complex amplitudes $\{E_x(x, y); E_y(x, y)\}$ of the object field of the polymer film is performed.

The technique of polarization-correlation determination of the distributions of the polarization ellipticity consists in the following set of actions:

1. Formation of planar polarization states in ‘irradiating’ and ‘reference’ laser beams.

ISSN 2077-7264. Технологія і техніка друкарства. 2022. № 2(76)

ISSN 2077-7264. Технологія і техніка друкарства. 2022. № 2(76)

2. Registration of two partial interference patterns through the polarizer-analyzer 14 with the orientation of the transmission plane at angles $\Omega = 0°$; $\Omega = 90°$.

3. For each partial interference distribution, we perform a two-dimensional discrete Fourier transform DFT(υ, ν) on the image. The two-dimensional DFT(υ, ν) of a two-dimensional array $I_{\Omega=0°;90°}(x, y)$ (i.e. the image) is a function of two discrete variables coordinates (x, y) is defined by [10]:

$$DFT_{\Omega=0^0;90^0}(\upsilon,\nu) = \frac{1}{M\times N}\sum_{x=0}^{M-1}\sum_{y=0}^{N-1} I_{\Omega=0^0;90^0}(x,y)\exp\left[-i2\pi\left(\frac{x\times\upsilon}{M}+\frac{y\times\nu}{N}\right)\right], \quad (1)$$

where $I_{\Omega=0^0;90^0}(x,y)=A_{\Omega=0^0;90^0}(x,y)A^*_{\Omega=0^0;90^0}(x,y)$

are the coordinate distributions of the intensity of the interference pattern filtered by the analyzer with the orientation of its transmission axis at $\Omega = 0°$; $\Omega = 90°$; $A_{\Omega=0°;90°}(x, y)$ are the orthogonal projections of the complex amplitudes; * denotes the complex conjugation operation; (υ, ν) are the spatial frequencies in the x and y directions respectively; and (M, N) are the number of pixels of the CCD camera in the x and y directions respectively, such that $0 \le x, \upsilon \le M$ and $0 \le y, \nu \le N$.

Results

The results of this transformation should contain three peaks, one central (main) peak and two additional side peaks. DFT in the described case works like a low-pass filter. It removes carrier (interference fringes) which is used to extract complex representation of real field from object. Also, since the extracted part has limited size, it also acts like a low-pass filter for the object field too.

Either of the additional side peaks (in complex representation) can be used to create a new Fourier spectrum by first extracting the peak and then placing it into centre of a newly generated spectrum $DFT_{\Omega=0°;90°}(\upsilon, \nu)$.

Applying a two-dimensional inverse discrete Fourier transform $(DFT_{\Omega=0°;90°})^*(x, y)$ on the obtained spectrum $DFT_{\Omega=0°;90°}(\upsilon, \nu)$, one gets:

$$\left(DFT_{\Omega=0^0;90^0}\right)^*(x,y) = \frac{1}{M\times N}\sum_{x=0}^{M-1}\sum_{y=0}^{N-1} DFT_{\Omega=0^0;90^0}(\upsilon,\nu)\exp\left[-i2\pi\left(\frac{x\times\upsilon}{M}+\frac{y\times\nu}{N}\right)\right]. \quad (2)$$

Here, $(DFT_{\Omega=0°;90°})^*(x,y) \equiv A_{\Omega=0°;90°}(x,y)$.

One subsequently obtains (for each state of polarization {Ir – Re}) a distribution of complex amplitudes:

$$\begin{cases}\Omega_{0^0}\to|A_0|;\\ \Omega_{90^0}\to|A_{90}|\exp\left(i\left(\delta_{90^0}-\delta_{0^0}\right)\right)\end{cases} \quad (3)$$

in different phase planes.

The phase planes are defined by:

$$\theta_k=\left(\delta_{90^0}-\delta_{0^0}\right)=\frac{2\pi}{\lambda}\Delta nz;$$

$$0 \le z \le h, \quad (4)$$

where Δn is the birefringence; λ is the wavelength; and h is the sample thickness of the object field, separated by an arbitrary step of $\Delta\theta$.

In each phase plane θ_k the corresponding sets of and polarization parameters (ellipticity β) of the object field of the layer are calculated:

$$\begin{aligned} S_1\left(0^0,90^0,45^0,\otimes\right) &= |E_x|^2+|E_y|^2;\\ S_2\left(0^0,90^0,45^0,\otimes\right) &= |E_x|^2-|E_y|^2;\\ S_3\left(0^0,90^0,45^0,\otimes\right) &= 2\mathrm{Re}\left|E_xE_y^*\right|;\\ S_4\left(0^0,90^0,45^0,\otimes\right) &= 2\mathrm{Im}\left|E_xE_y^*\right|. \end{aligned} \quad (5)$$

Here 0°, 90°, 45° — polarization azimuths of linearly polarized irradiating beams, ⊗ — right circularly polarized beam.

Further, based on relations (1), the set of elements of the Mueller matrix is calculated using the following Stokes-polarimetric relations:

$$\{M\}=0{,}5\begin{Vmatrix} (S_1^0+S_1^{90}) & (S_1^0-S_1^{90}) & (S_1^{45}-S_1^{135}) & (S_1^{\otimes}-S_1^{\oplus}) \\ (S_2^0+S_2^{90}) & (S_2^0-S_2^{90}) & (S_2^{45}-S_2^{135}) & (S_2^{\otimes}-S_2^{\oplus}) \\ (S_3^0+S_3^{90}) & (S_3^0-S_3^{90}) & (S_3^{45}-S_3^{135}) & (S_3^{\otimes}-S_3^{\oplus}) \\ (S_4^0+S_4^{90}) & (S_4^0-S_4^{90}) & (S_4^{45}-S_4^{135}) & (S_4^{\otimes}-S_4^{\oplus}) \end{Vmatrix}. \quad (6)$$

Traditionally, on the right side of expressions (2), the value of the phase shift $\delta(z = l)$ integral over the entire thickness l of the layer 'appears'.

Therefore, the results of direct Mueller-matrix mapping are two-dimensional distributions of the values of matrix elements $M_{ik} = q_j(S_{z=1;2;3;4}(x,y,\delta))$ averaged $(d(z = l))$ over the entire thickness l of the polymer film.

In the case of using a coherent reference wave and digital holographic reproduction algorithms, it becomes possible to reproduce the distributions of the complex amplitudes $|E_x|\exp i(\Delta\delta_x)$; $|E_y|\exp i(\Delta\delta_y)$ of the object field in a discrete $(\Delta\delta_{l=0\ldots q})$ set of phase planes $\delta=\begin{pmatrix} 0 \\ \Delta\delta \\ 2\Delta\delta \\ \vdots \\ \delta \end{pmatrix}$. Due to this, it is possible to obtain a set of layer-by-layer distributions of the magnitude of matrix elements (x, y, kΔδ) and determine their volumetric structure

$$M_{ik}=\left\{g_s\left(|E_x|,|E_y|,\delta^*\right)\right\}\left(x,y,\begin{pmatrix} 0 \\ \Delta\delta \\ \vdots \\ \delta \end{pmatrix}\right). \quad (7)$$

In fig. 1 are shown the optical arrangement of the 3D Mueller-matrix polarimetry of the polymer film.

Parallel ($\varnothing = 2\times10^3$ μm) beam of He-Ne (λ = 0,6328 μm) laser *1*, formed with collimator *2*, with 50 % beam splitter *3*, is divided into 'irradiating' and 'reference'.

Parallel beam of He-Ne laser *1*, formed by spatial-frequency filter *2*, with 50/50 beam splitter *5* is divided into 'object' and 'reference' ones. The input polarization state formed by quarter wave plate *3* and polarizer *4* is linear with azimuth 00 (perpendicular) with respect to the XY plane.

The 'object' beam with the help of a rotating mirror *8* is directed through the polarizing filter *9–11* in the direction of the sample of the biological layer *15*. The polarization-inhomogeneous image of the object *15* is projected by the strain-free objective *17* into the plane of the digital camera *18*.

The 'reference' beam is directed by the mirror *7* through the polarization filter *12–14* into the plane of the polarization-inhomogeneous image of the object *15*.

As a result, an interference pattern is formed, the coordinate intensity distribution of which is recorded by a digital camera *18*.

The technique of polarization-interference determination of the elements of the Mueller matrix consists in the following set of actions:

Formation of six polarization states in the irradiating and reference laser beams — (0° – 0°); (90° – 90°); (45° – 45°); (135° – 135°); (⊗ – ⊗); (⊕ – ⊕).

Registration of each partial interference pattern through the polarizer-analyzer *14* with sequential

ISSN 2077-7264. Технологія і техніка друкарства. 2022. № 2(76)

ISSN 2077-7264. Технологія і техніка друкарства. 2022. № 2(76)

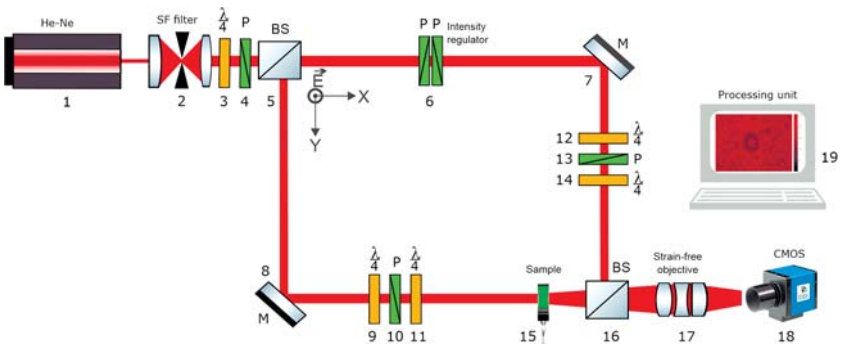

Fig. 1. Diagram of polarization interferometry of 3D distributions of the elements of the Mueller matrix. Explanations in the text

orientation of the transmission plane at angles Ω = 0°; Ω = 90°.

For an objective assessment of layer-by-layer polarization maps $S(\theta_k, x, y)$, the statistical moments of the first (z_1), second (z_2), third (z_3) and fourth (z_4) orders were used, which were calculated by the following algorithms [8]

$$Z_1 = \frac{1}{N}\sum_{j=1}^{N} S(\theta_k, x, y)_j;$$

$$Z_2 = \sqrt{\frac{1}{N}\sum_{j=1}^{N}\left(S^2(\theta_k, x, y)\right)_j};$$

$$Z_3 = \frac{1}{Z_2^3}\frac{1}{N}\sum_{j=1}^{N}\left(S^3(\theta_k, x, y)\right)_j; \quad (8)$$

$$Z_4 = \frac{1}{Z_2^4}\frac{1}{N}\sum_{j=1}^{N}\left(S^4(\theta_k, x, y)\right)_j,$$

where N — number of pixels of the photosensitive area of the CCD camera.

Discusion

To determine the optimal phase plane, we used a two-stage algorithm for analyzing layer-by-layer maps of the optical anisotropy.

1. At the first stage:

— Selected step of discrete phase 'macro' scanning $\Delta\theta_k^{max}=0.25\text{rad}$.

— Algorithmically reconstructed a series of corresponding to each $\Delta\theta_k^{max}=0.25\text{rad}$ layer-by-layer coordinate distributions of the magnitude of the $S(x, y, \theta_k)$.

— Statistical moments of the 1st–4th orders $Z_{i=1;2;3;4}$, which characterize the obtained 2D distributions $S(x, y, \theta_k)$, were calculated.

— The difference between the values of each of the statistical moments of the 1st–4th orders was calculated $(\Delta Z_i)_k = Z_i\left(\theta_{j+1}^{max}\right) - Z_i\left(\theta_j^{max}\right)$.

— The phase interval $\Delta\theta^* = \left(\theta_{j+1}^{max} \div \theta_j^{max}\right)$ was determined, within which the monotonic growth of the value $\Delta Z_i = Z_i\left(\theta_{j+1}^{max}\right) - Z_i\left(\theta_j^{max}\right) \le 0$ stops.

— Within the limits $\Delta\theta^*$, a new series $\Delta Z_i = Z_i\left(\theta_{q+1}^{min}\right) - Z_i\left(\theta_q^{min}\right)$ of values was calculated with a discrete phase 'micro' scan step $\Delta\theta_q^{min}=0.05\text{rad}$.

— The optimal phase plane θ^* was determined, in which $\Delta z_i(\theta^*) = \max$.

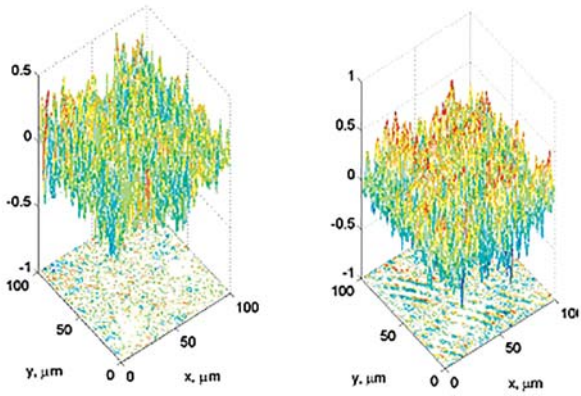

Fig. 2. 3D maps of distributions of linear birefringence (left side) and dichroism (right side) of a partially depolarizing polycrystalline film

Calculations of the distributions of optical anisotropy parameters (fig. 2).

Conclusions

1. A method for 3D Muller-matrix reproduction of the distributions of the parameters of linear and circular birefringence and dichroism of partially depolarizing polycrystalline films is proposed and substantiated.

2. The dynamics of the change in the value of the statistical moments of the 1st–4th orders, characterizing the distributions of the optical anisotropy parameters of a polycrystalline polymer film in various 'phase' sections of its volume, has been investigated and analyzed.

References

1. Mishchenko, M. I., Travis, L. D., & Lacis, A. A. (2002). *Scattering, Absorption, and Emission of Light by Small Particles*. Cambridge University Press, Cambridge.

2. Swami, M. K., Patel, H. S., & Gupta, P. K. (2013). Conversion of 3×3 Mueller matrix to 4×4 Mueller matrix for non-depolarizing samples. *Opt. Commun*, 286(1), 18–22.

3. Izotova V. F., & et al. (1997). Investigation of Mueller matrices of anisotropic nonhomogeneous layers in application to optical model of cornea. *Appl. Opt.*, 36(1), 164–169.

4. Tuchin, V. V. (2015). Tissue optics and photonics: biological tissue structures [review]. *J. Biomed. Photonics Eng.*, 1(1), 3–21.

5. Tuchin, V. V. (2015). Tissue optics and photonics: light-tissue interaction [review]. *J. Biomed. Photonics Eng.*, 1(2), 98–134.

6. Manhas, S., & et al. (2006). Mueller matrix approach for determination of optical rotation in chiral turbid media in backscattering geometry. *Opt. Express*, 14(1), 190–202.

7. Deng, Y., & et al. (2007). Characterization of backscattering Mueller matrix patterns of highly scattering media with triple scattering assumption. *Opt. Express*, 15(15), 9672–9680.

ISSN 2077-7264. Технологія і техніка друкарства. 2022. № 2(76)

8. Ushenko, A. G., & Pishak, V. P. (2004). *Laser Polarimetry of Biological Tissue: Principles and Applications*. in Handbook of Coherent-Domain Optical Methods: Biomedical Diagnostics, Environmental and Material Science, vol. I, Ed. Tuchin, V. V. Boston: Kluwer Academic Publishers, pp. 93–138.

9. Angelsky, O. V., Ushenko, A. G., Ushenko, Yu. A., Pishak, V. P., & Peresunko, A. P. (2010). *Statistical, Correlation and Topological Approaches in Diagnostics of the Structure and Physiological State of Birefringent Biological Tissues.* in Handbook of Photonics for Biomedical Science, pp. 283–322. Ed. by Tuchin, V. V. CRC PressTaylor&Francis group: Boca Raton, London, New York.

10. Ushenko, Y. A., Boychuk, T. M., Bachynsky, V. T., & Mincer, O. P. (2013). *Diagnostics of Structure and Physiological State of Birefringent Biological Tissues: Statistical, Correlation and Topological Approaches*. in Handbook of Coherent-Domain Optical Methods, Springer Science+Business Media, p. 107, New York.

У статті аналітично узагальнено вектор-параметричну та Мюллер-матричну поляриметрію оптично анізотропних фазово-неоднорідних шарів з полікристалічною архітектонікою.

Ключові слова: 3D реконструкція; полімерна плівка; матриця Мюллера; деполяризація.

Надійшла до редакції 07.09.22